ApoER2/VLDL receptor and Dab1 in the rostral migratory stream function in postnatal neuronal migration independently of Reelin

Nuno Andrade*, Vukoslav Komnenovic†, Sophia M. Blake*, Yves Jossin‡, Brian Howell§, Andre Goffinet‡, Wolfgang J. Schneider*, and Johannes Nimpf*¶

*Max F. Perutz Laboratories, University Departments at the Vienna Biocenter, Department of Medical Biochemistry, Medical University of Vienna, A-1030 Vienna, Austria; †Institute of Molecular Biotechnology, Austrian Academy of Sciences, 1030 Vienna, Austria; ‡Developmental Neurobiology Unit, University of Leuven Medical School, 3000 Leuven, Belgium; and §Neurogenetics Branch, National Institute of Neurological Disorders and Stroke, National Institutes of Health, Bethesda, MD 20892

Edited by Thomas C. Südhof, The University of Texas Southwestern Medical Center, Dallas, TX, and approved March 30, 2007 (received for review December 21, 2006)

Postnatal migration of interneuron precursors from the subventricular zone to the olfactory bulb occurs in chains that form the substrate for the rostral migratory stream. Reelin is suggested to induce detachment of neuroblasts from the chains when they arrive at the olfactory bulb. Here we show that ApoER2 and possibly very-low-density lipoprotein receptor (VLDLR) and their intracellular adapter protein Dab1 are involved in chain formation most likely independent of Reelin. F-spondin, which is present in the stream, may act as ligand for ApoER2 and VLDLR. In mice lacking either both receptors or Dab1 chain formation is severely compromised, and as a consequence the rostral migratory stream is virtually absent and neuroblasts accumulate in the subventricular zone. The mutant animals exhibit severe neuroanatomical defects in the subventricular zone and in the olfactory bulb. These data demonstrate a cell-autonomous function of ApoER2, and most likely VLDLR and Dab1, in postnatal migration of neuroblasts in the forebrain, which is suggested to depend on ligands other than Reelin.

Reelin signaling | postnatal neurogenesis | tangential neuronal migration

The development of the olfactory bulb (OB) in rodents continues after birth. Most interneurons differentiate from neuroblasts generated postnatally in the subventricular zone (SVZ) of the cerebral cortex and migrate to the OB along the so-called "rostral migratory stream" (RMS) (1). Whereas the majority of these neuroblasts originate and migrate during the early postnatal period, the process continues throughout life (2). Neuronal migration in the RMS occurs by formation of chains that are ensheathed by glial cells and their processes (3). In these chains, neuroblasts migrate along each other in a saltatory fashion (4).

Migration along the RMS depends on the transcription factor serum response factor (SRF) (5). In the absence of SRF, cells destined for the OB accumulate in the SVZ because of a cell-autonomous defect that might be caused by down-regulation of actin and gelsolin, impairing the dynamics of actin microfilaments. The polysialylated form of neural cell adhesion molecule (NCAM) (6) mediates the interaction between migrating neuroblasts and their environment (7, 8). Migration in the RMS is guided by the repulsive action of Slit secreted by cells in the lateral septum and the SVZ (9, 10), as well as by Netrin (11). Once in the OB, neuroblasts switch from chain migration to radial migration, integrate into the laminated structure of the bulb, and differentiate into granule and periglomerular interneurons (2, 12). The switch from chain migration to radial migration seems to depend on the Reelin signal that detaches neuroblasts from the chains (13). Reelin is expressed by olfactory mitral cells (14), and Reelin-deficient mice have a diminutive OB because of a reduction of the number of neurons and a disorganization of the granular cell layer (Gcl) (15). Thus, it seems that Reelin also orchestrates the lamination of the OB, as it does in the cerebrum and other laminated structures (for reviews see refs. 16 and 17).

In the cerebrum, Reelin is crucial for correct positioning of radially migrating neuroblasts via its binding to ApoER2 and very-low-density lipoprotein receptor (VLDLR) (18, 19), which triggers tyrosine phosphorylation of the adaptor Dab1 by receptor clustering (20). Binding of Reelin to the receptors and subsequent phosphorylation of Dab1 are consecutive steps of a linear pathway, because disruption of any of the corresponding genes causes identical phenotypes in mice (21–24).

Here we report that the lack of ApoER2/VLDLR or Dab1 leads to a cell-autonomous migration defect in the RMS, which is independent of the Reelin signal. Neuroblasts from mutant mice lacking either receptors or Dab1 are unable to form chains and accumulate in the SVZ. As a consequence, the RMS is missing or is very rudimentary. This leads to severe neuroanatomical defects in the SVZ and in the OB of mutant animals. Reelin is not present in the stream and does not play a role in chain formation, but it seems to be involved in maintenance or architecture of the RMS. F-spondin might be a candidate ligand for ApoER2 and VLDLR in the RMS.

Results

ApoER2 and VLDLR and the associated machinery that transduces the Reelin signal play major roles in allowing neuroblasts to switch from chain migration to tangential migration within the OB (13). Neuroblasts within the RMS expressed the ApoER2 protein (Fig. 1 *A* and *B*), confirming *in situ* hybridization data (13). ApoER2 expression was already prominent in neuroblasts generated in the SVZ (Fig. 1 *A* and *C*, open arrowheads), long before they reach the bulb where the Reelin signal is generated (13). The ApoER2-positive staining is specific, because it is absent in mice deficient in ApoER2 and VLDLR (Fig. 1*D*). Close inspection of these mice, however, indicated that the RMS was absent. To evaluate this further, we examined the RMS in WT mice and mice lacking defined components of the Reelin pathway. Sagittal sections of brains from mice at postnatal day 17 (P17) were stained with hematoxylin and with an antibody against doublecortin, a marker

Author contributions: N.A. and J.N. designed research; N.A., V.K., S.M.B., and Y.J. performed research; B.H. contributed new reagents/analytic tools; N.A., Y.J., B.H., A.G., and W.J.S. analyzed data; and A.G. and J.N. wrote the paper.

The authors declare no conflict of interest.

This article is a PNAS Direct Submission.

Abbreviations: SRF, serum response factor; RMS, rostral migratory stream; SVZ, subventricular zone; OB, olfactory bulb; EZ, ependymal zone; Gcl, granular cell layer; VLDLR, very-low-density lipoprotein receptor; P*n*, postnatal day *n*.

¶To whom correspondence should be addressed. E-mail: johannes.nimpf@meduniwien.ac.at.

This article contains supporting information online at www.pnas.org/cgi/content/full/0611391104/DC1.

www.pnas.org/cgi/doi/10.1073/pnas.0611391104

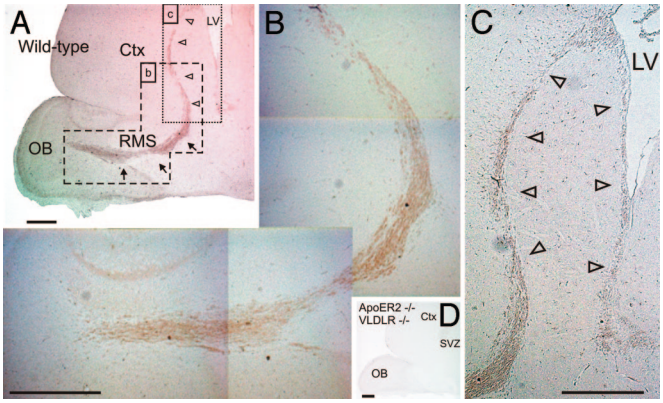

Fig. 1. Neuroblasts migrating within the RMS express ApoER2. Sagittal sections (5 μm) of the forebrains of WT mice (*A–C*) and from *ApoER2*$^{-/-}$/*VLDLR*$^{-/-}$ mice (*D*) were immunostained with a polyclonal antibody against ApoER2. The RMS is highlighted by arrows, and the SVZ is highlighted by open arrowheads. Ctx, cortex; LV, lateral ventricle; St, striatum. (Scale bars: 500 μm.)

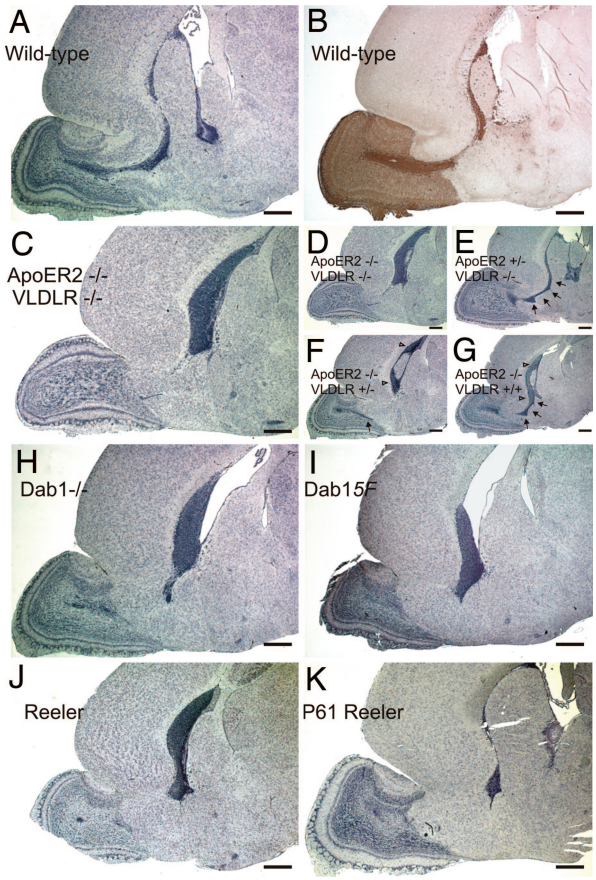

Fig. 2. Ablation of critical components of the Reelin signaling pathway leads to loss of the RMS and accumulation of neuroblasts in the SVZ. Sagittal sections (5 μm) of the forebrains of WT (*A* and *B*), *ApoER2*$^{-/-}$/*VLDLR*$^{-/-}$ (*C* and *D*), *ApoER2*$^{+/-}$/*VLDLR*$^{-/-}$ (*E*), *ApoER2*$^{-/-}$/*VLDLR*$^{+/-}$ (*F*), *ApoER2*$^{-/-}$/*VLDLR*$^{+/+}$ (*G*), *Dab1*$^{-/-}$ (*H*), *Dab1-5F* (*I*), and *reeler* (*J*) mice at P17 and *reeler* mice (*K*) at P61 were stained with hematoxylin (*A* and *C–K*) or with an antibody against doublecortin (*B*). Sections were taken from three to five independent animals from each of the genetic backgrounds, and representative sections are displayed. (Scale bars: 500 μm.) Arrows are used to highlight the RMS.

of the RMS (25); for the mutant animals only sections stained with hematoxylin are shown. In WT mice, a well defined stream of neuroblasts started at the SVZ and ended within the OB defining the RMS (Fig. 2 *A* and *B*). In mice lacking ApoER2 and VLDLR (Fig. 2*C*), Dab1 (Fig. 2*H*), carrying two Dab1 alleles (*Dab1-5F*) in which the critical tyrosine residues are mutated to phenylalanines instead of the WT alleles (26) (Fig. 2*I*), or functional Reelin (Fig. 2*J*), the RMS was severely disrupted and neuroblasts accumulated in the SVZ. The cells accumulating in the SVZ of *reeler* mice and *Dab1*$^{-/-}$ mice still expressed ApoER2 [see supporting information (SI) Fig. 8]. The lack of an RMS seen in *reeler* mice was surprising, because in a previous study a stream that was fanning out just before it reaches the OB was observed in these mice (13). To exclude the possibility that the age of the mice examined made the difference, we also looked at P61 (Fig. 2*K*). Again no stream could be detected, but the accumulation of neuroblasts in the SVZ was less prominent. Serial sagittal sections (5 μm) through the area that would contain the entire RMS revealed that in all mutant animals some patches or solitary individual neuroblasts can be identified migrating from the SVZ toward the OB (data not shown).

Whereas ApoER2 was expressed by neuroblasts in the RMS (Fig. 1), VLDLR was not detected in this structure by *in situ* hybridization (13) or by using a specific antibody (data not shown). Allelic titration of both receptors, however, suggested the presence of VLDLR within the RMS. The presence of one *Apoer2* allele on a *Vldlr*-null background was sufficient to develop an RMS and a SVZ that were indistinguishable from that of WT mice (Fig. 2*E* and SI Fig. 9*B*). The presence of one *Vldlr* allele on an *Apoer2*-null background partially rescued the "RMS-less" phenotype (Fig. 2*F*, black arrow): a faint RMS could be detected by serial sagittal sections. The presence of two WT *Vldlr* alleles almost reestablished the RMS (Fig. 2*G*). Most of the stream was restored, but some neuroblasts still accumulated in the SVZ (SI Fig. 9*D*).

The accumulation of neuroblasts in the SVZ of mice lacking functional Reelin, ApoER2/VLDLR, or Dab1 was also evident in coronal sections (see SI Fig. 10). In comparison to WT mice, where the SVZ appeared as a narrow band of cells, in mutant animals this zone was significantly wider and densely packed with neuroblasts.

To investigate whether the lack of RMS formation also caused accumulation of glial cells in the SVZ, we performed double-staining for GFAP and doublecortin. Numerous GFAP-positive cells were present in the region where neuroblasts accumulated in the mutant mice (SI Fig. 11), indicating that not only neuroblasts, but also accompanying glial cells, accumulated in the SVZ when no RMS was formed. TUNEL analysis disclosed the presence of apoptotic cells within the mass of accumulating neuroblasts (Fig. 3). A 15-fold increase of apoptotic cells was found in the mutant SVZs compared with the WT SVZ (five to eight matched sections from three different animals for each genotype: WT, 0.22 ± 0.2%; *reeler*, 3.42 ± 0.5%; *ApoER2*$^{-/-}$/*VLDLR*$^{-/-}$, 3.56 ± 0.9%; *Dab1*$^{-/-}$, 3.6 ± 1%; ***, $P < 0.0005$). There was no significant difference in apoptosis among the mutant SVZs ($P > 0.1$).

To define the impact of the loss of the RMS on the structure of the OB, we analyzed the mature bulbs of the respective mutant mice. First, we prepared coronal sections as schematized in Fig. 4*J* and estimated the number of cells present in the Gcl including the ependymal zone (EZ) on hematoxylin-stained sections (Fig. 4*I*). The structure of the WT bulb is characterized, from the center to the periphery, by a cell-dense center (EZ), followed by the Gcl, separated from the external plexiform layer by a well defined layer of mitral cells (27). The outermost structure is the glomerular layer that contains calretinin- and calbindin-positive neurons derived from the RMS (1). Hematoxylin (Fig. 4*A*) and immunohistochemical staining for ApoER2 (Fig. 4*E*) of a WT OB confirmed expression of ApoER2 in mitral cells (14) and demonstrated that most cells present in the EZ were immunopositive for ApoER2 (compare to Fig. 1), indicating that these cells derived from the RMS. The OBs from *reeler*, *ApoER2*$^{-/-}$/*VLDLR*$^{-/-}$, and *Dab1*$^{-/-}$ mice contained only 60% of the number of cells in the Gcls

NEUROSCIENCE

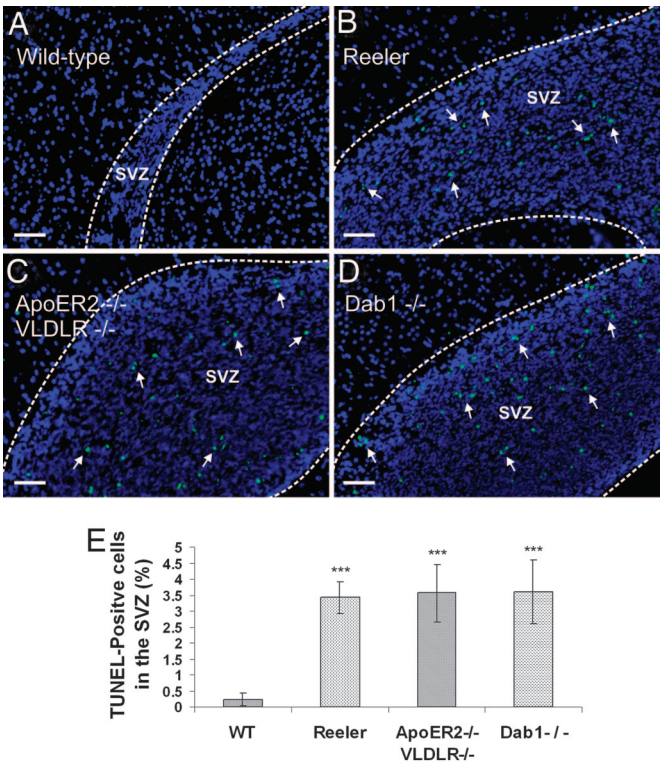

Fig. 3. Cell accumulation in the SVZs of *reeler*, *ApoER2*$^{-/-}$/*VLDLR*$^{-/-}$, and *Dab1*$^{-/-}$ mice leads to increased apoptosis. Sagittal sections (5 μm) prepared from the forebrains of WT (*A*), *reeler* (*B*), *ApoER2*$^{-/-}$/*VLDLR*$^{-/-}$ (*C*), and *Dab1*$^{-/-}$ (*D*) mice were analyzed for the presence of apoptotic cells by TUNEL assays. (*E*) Apoptosis was quantified based on the percentage of TUNEL-positive cells in the SVZ using five to eight matched 5-μm sections from three animals from each genetic background. Plots show average ± SEM. ***, $P <$ 0.0005 (Student's *t* test). (Scale bars: 50 μm.)

compared with their WT counterparts (Fig. 4*I*) (Number of cells in the granular zone in 5-μm sections from two to three animals per background was normalized to the WT values: WT, 1.00 ± 0.07; *reeler*, 0.59 ± 0.05; *ApoER2*$^{-/-}$/*VLDLR*$^{-/-}$, 0.59 ± 0.1; *Dab1*$^{-/-}$ 0.58 ± 0.06; ***, $P <$ 0.0005). This effect was mostly due to a dramatic reduction of cells present in the mutant EZs. This finding was confirmed by BrdU staining. Animals were injected with BrdU at P12, and the SVZ and the OBs were analyzed at P17. In WT mice, the EZ of the OB was filled with BrdU-positive cells (Fig. 5*A*), and the corresponding SVZ was represented by a thin layer of neuroblasts (Fig. 5*a*). In *reeler*, *ApoER2*$^{-/-}$/*VLDLR*$^{-/-}$, and *Dab1*$^{-/-}$ mice, the BrdU-positive staining was dramatically reduced in the EZ of the bulb (Fig. 5 *B–D*) and increased in the respective SVZs (Fig. 5 *b* and *c*). Quantification of calbindin- and calretinin-positive cells (SI Fig. 12) in the glomerular layers disclosed a 3-fold reduction of calbindin-positive cells per glomerulus and an ≈2-fold reduction of calretinin-positive cells in all mutant animals.

To evaluate whether a migration defect was responsible for the lack of the RMS, migration assays in three-dimensional extracellular matrix substrate (Matrigel) of SVZ explants were performed to study chain formation and tangential migration of neuroblasts *in vitro* (4). For quantification of the effects, the average migration distance (length of chains) was measured (Fig. 6*F*), and the number of individual cells per field was counted (Fig. 6*G*). Explants from WT mice extended robust chains consisting of migrating neuroblasts and glial cells (4), which, after 50 h, reached an average length of 262 ± 27 μm (Fig. 6*A*). Under these conditions, very few individual neurons (11.4 ± 7) were present around the explant. Addition of Reelin caused disintegration of the chains, confirming previous observations (13) (data not shown). Chain development and neuronal migration in explants from *reeler* mice (Fig. 6*B*) were indistinguishable from those seen in WT mice (chain length: 266 ± 19 μm; WT, $n = 19$; *reeler*, $n = 16$; explants from at least two animals per genotype; $P > 0.1$), suggesting that Reelin is not crucial for the formation of the chains or for the migration of the cells in chains. In sharp contrast, the development of explants cultured from *ApoER2*$^{-/-}$/*VLDLR*$^{-/-}$ mice was dramatically different (Fig. 6*C*). Only a few neurons left the explants, and the few chains formed were dramatically shorter than those in explants from WT or *reeler* mice (107 ± 47 μm, $n = 20$ explants from two mice; ***, $P < 0.0005$). Explants from *Dab1*$^{-/-}$ mice (Fig. 6*D*) and *Dab1-5F* mice (data not shown) also developed differently from WT explants. A significant number of neurons migrated out and away from the explant, but most of them failed to form chains. These experiments demonstrated that the lack of RMS formation in *reeler* mice is not due to a migration defect of neuroblasts. In mice lacking either ApoER2/VLDLR or Dab1, the absence of the RMS is caused by a migration defect and/or by the inability of neuroblasts to form chains. To define whether this is a cell-autonomous defect, explants from WT animals were infected with an adenovirus to express EGFP and were cocultured with explants derived from *ApoER2*$^{-/-}$/*VLDLR*$^{-/-}$ mice. As demonstrated in Fig. 6*E*, the presence of the WT explant did not induce *ApoER2*$^{-/-}$/*VLDLR*$^{-/-}$ neuroblasts to migrate out of the explant and to form chains. These results demonstrated that the lack of ApoER2 and VLDLR caused a cell-autonomous migration defect that is independent of the presence of Reelin. To support this view, we examined the RMS of WT and *reeler* mice (data not shown) for the presence of Reelin-expressing cells. The *reeler-Orleans* mutant mice used in this study produce a truncated Reelin protein that is not secreted from cells and thus can be readily detected by immunostaining (28). As demonstrated in Fig. 7, we confirmed previous findings that Reelin-expressing cells are present neither at the origin of nor within the RMS (13, 29). However, areas adjacent to the stream contained a significant number of Reelin-producing cells.

What is the ligand for ApoER2 and VLDLR within the stream? Because VLDLR and ApoER2 are promiscuous receptors (30), we tested other ligands for their presence in the RMS. To this end, we could demonstrate that F-spondin, which was recently identified as a ligand for ApoER2 (31), is indeed present in the RMS as shown by immunohistochemistry (Fig. 7*B*). This result was in agreement with the genome-wide *in situ* hybridization results presented in the Allen Brain Atlas (32). The specificity of the staining is further documented by examination of *ApoER2*$^{-/-}$/*VLDLR*$^{-/-}$ mice (Fig. 7*C*). Here F-spondin is confined to the area of accumulating cells destined to form the RMS.

As outlined in the Introduction, mice lacking the gene for SRF exhibit a similar phenotype most likely due to the down-regulation of actin and gelsolin. Thus, we tested whether actin and gelsolin are reduced in the forebrains of our mutants. As demonstrated in SI Fig. 13, the expression levels of actin and gelsolin are not significantly affected in *reeler*, *ApoER2*$^{-/-}$/*VLDLR*$^{-/-}$, or *Dab*$^{-/-}$ mice compared with WT mice.

Discussion

Development of the OB in mice in part depends on postnatal neurogenesis taking place in the SVZ. Tangential migration of neuroblasts along the RMS ensures the integration of these cells into structures of the OB. This mode of migration is characterized by the formation of chains containing migrating neuroblasts and supporting glial cells. Here we have identified ApoER2 and VLDLR as major components of the cellular machinery that supports formation of the chains. In our hands the lack of Dab1 also compromises the formation of chains, which is in contrast to a previous notion (33). Because explants from *Dab1-5F* mice

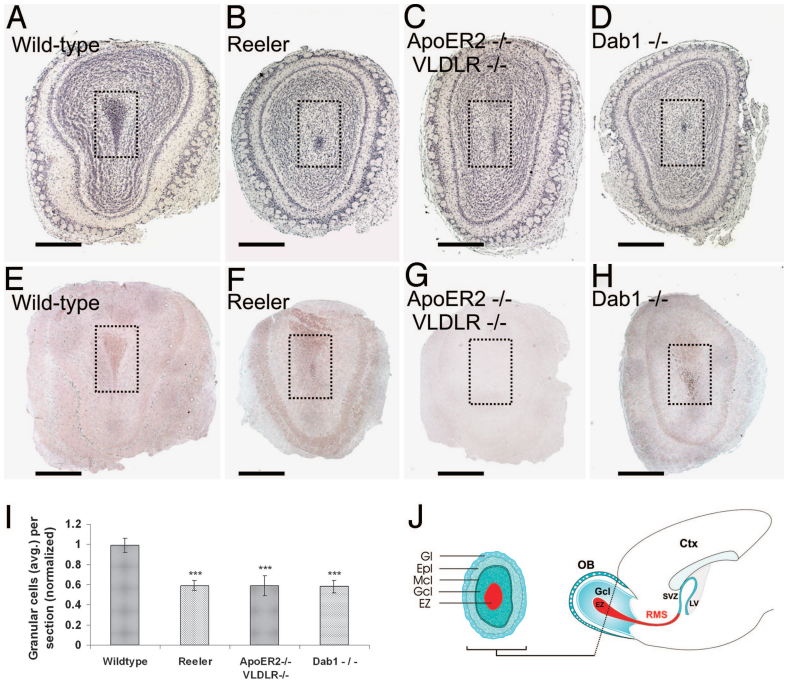

Fig. 4. OBs from *reeler* mice, *ApoER2*$^{-/-}$/*VLDLR*$^{-/-}$ mice, and *Dab1*$^{-/-}$ mice have a reduced or vestigial EZ. Matched coronal sections (5 μm) derived from the OBs of WT mice (*A* and *E*), *reeler* mice (*B* and *F*), *ApoER2*$^{-/-}$/*VLDLR*$^{-/-}$ mice (*C* and *G*), and *Dab1*$^{-/-}$ mice (*D* and *H*) were stained with hematoxylin (*A–D*) or immunostained for ApoER2 (*E–H*). The EZ (darker area inside the doted squares) is drastically reduced in the mutant OBs because of the disruption of the corresponding RMS (*B–D*). (*I*) Quantification of the cell numbers present in the Gcl and EZ (normalized to the cell number in the Gcl of WT mice) displayed a 40% decrease in the mutant OBs. Average cell numbers were calculated from 11 matched sections from two WT mice, 19 matched sections from three *reeler* mice, 18 matched sections from three *ApoER2*$^{-/-}$/*VLDLR*$^{-/-}$ mice, and 18 matched sections from three *Dab1*$^{-/-}$ mice. Plots show average ± SEM. ***, $P < 0.0005$ (Student's *t* test). (*J*) Schematic illustration of a coronal section from an OB (*Left*) and a sagittal section of a forebrain (*Right*). (Scale bars: 500 μm.) Ctx, cortex; LV, lateral ventricle.

have a similar phenotype we are proposing that the whole complex comprising the receptors and Dab1 is involved in chain formation. In mice lacking either both receptors or Dab1, chain formation in the SVZ is defective without compromising the generation of neuroblasts in the SVZ. This leads to an ectopic accumulation of neuroblasts and glial cells in the SVZ accompanied by a significant increase of cell death. For two reasons this defect cannot be due to interference with the classical Reelin signaling pathway: first, SVZ explants derived from *reeler* mice produced chains indistinguishable from those in WT explants; second, activation of the pathway by Reelin *in vitro* leads to disintegration of the chains (13).

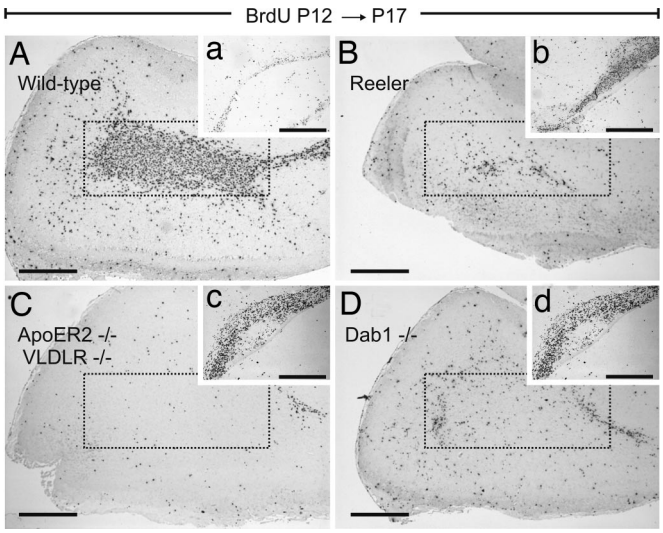

Fig. 5. Migration of newly generated neuroblasts is affected in the forebrains of mice carrying mutations in the Reelin signaling pathway. WT (*A*), *reeler* (*B*), *ApoER2*$^{-/-}$/*VLDLR*$^{-/-}$ (*C*), and *Dab1*$^{-/-}$ (*D*) mice received a BrdU pulse at P12, and brains were collected at P17. Matched sagittal sections of the forebrains were stained for BrdU-positive cells. Areas corresponding to the EZs are marked by dotted frames. (*a–d*) BrdU staining of the corresponding SVZs. (Scale bars: 500 μm.)

Interestingly, the RMS of *reeler* mice is affected similarly, and the observed phenotype seems to be more severe than previously described (13). There, the *reeler* RMS was found to be normal from its origin at the SVZ until shortly before it reaches the entrance point of the OB, where it became wider and less defined. This difference is presumably neither due to differences in genetic backgrounds, because the same strain of *reeler* mutants was used in both studies, nor related to the different ages of the animals analyzed (adult animals versus P17 in our study), because in *reeler* mice at P61 still no RMS could be found, although accumulation of neuroblasts in the SVZ was significantly reduced compared with P17, most likely because of apoptosis.

These results suggest a subdivision of the RMS formation into four mechanistically distinct phases. First is formation of neuroblasts and accompanying glial cells in the SVZ from respective precursor cells. This does not seem to be compromised by the lack of Reelin or the "receptor/adapter" machinery. Second is formation of chains, the substrate for the specific mode of neuronal migration within the RMS. This step depends on the presence of the receptor/adapter machinery but is independent of Reelin, because regular chains are formed by *reeler* explants in *vitro*. Third is bundling of the chains into a stream, and fourth is maintenance and elongation of a defined RMS, in which Reelin, expressed by cells in the vicinity of the stream, appears to play an important role. Whether the entire Reelin-signaling pathway is involved at this point cannot be answered from these

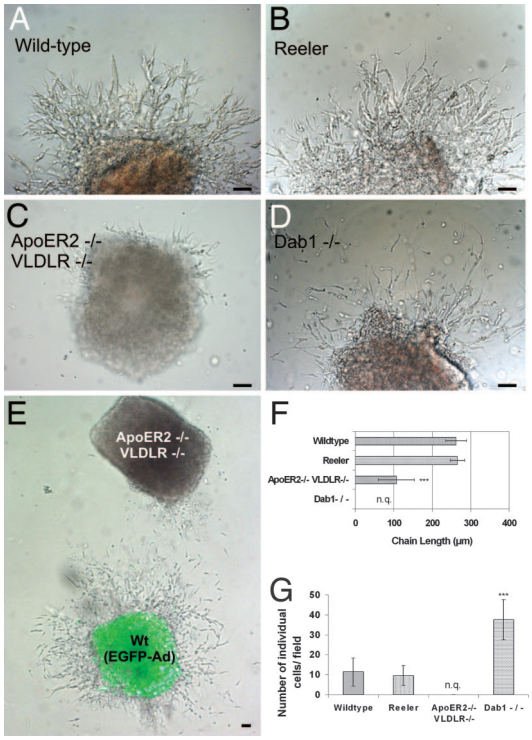

Fig. 6. Chain formation from explants of the SVZ is normal in *reeler* but severely disturbed in *ApoER2*$^{-/-}$/*VLDLR*$^{-/-}$ and *Dab1*$^{-/-}$ mice. SVZ explants were prepared from P5 WT (*A*), *reeler* (*B*), *ApoER2*$^{-/-}$/*VLDLR*$^{-/-}$ (*C*), and *Dab1*$^{-/-}$ (*D*) mice and analyzed after 50 h in culture by measuring the length of migratory chains (*F*, distance between the bases to the tips of the chains) and the number of individual cells per field (*G*). For quantification 19 WT, 16 *reeler*, 20 *ApoER2*$^{-/-}$/*VLDLR*$^{-/-}$, and 21 *Dab1*$^{-/-}$ explants from two mice of each phenotype were used. Plots show average ± SEM. ***, $P < 0.0001$ (Student's *t* test). (*E*) WT SVZ explants infected with EGFP adenovirus were cocultured with explants from *ApoER2*$^{-/-}$/*VLDLR*$^{-/-}$ mice. n.q., not quantified. (Scale bar: 50 μm.)

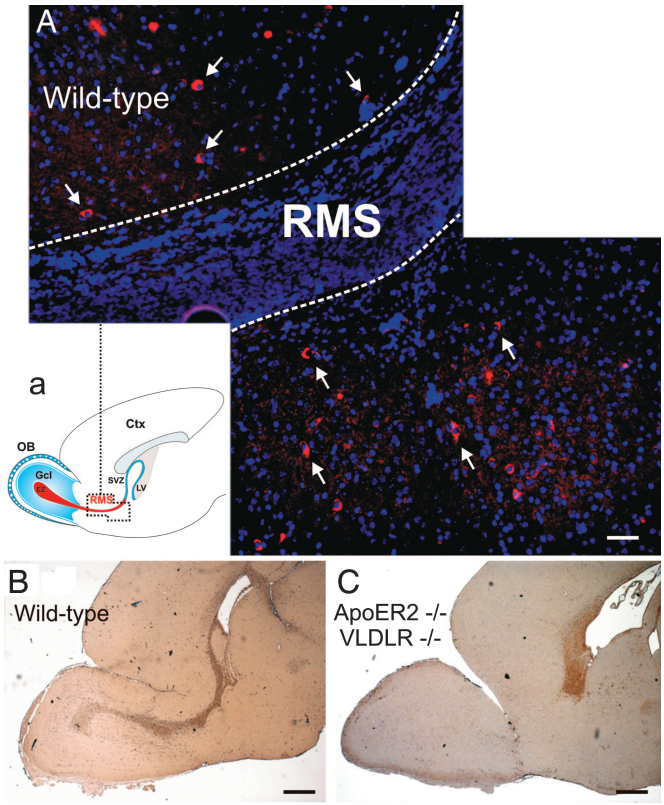

Fig. 7. Expression of Reelin and F-spondin in the RMS. (*A*) Reelin-positive cells accompany the RMS. Sagittal sections (5 μm) prepared from the forebrains of WT mice were immunostained with an antibody against Reelin. The RMS is highlighted by dotted lines. Reelin-positive cells are indicated by arrows. (*a*) Schematic representation of the area shown in *A*. (Scale bar: 50 μm.) (*B* and *C*) F-spondin is present in the RMS and accumulates in the SVZ of *ApoER2*$^{-/-}$/*VLDLR*$^{-/-}$ mice. Sagittal sections (5 μm) prepared from the forebrains of WT (*B*) and *ApoER2*$^{-/-}$/*VLDLR*$^{-/-}$ (*C*) mice were immunostained with an antibody against F-spondin. (Scale bar: 500 μm.)

experiments, because chains are not formed in *ApoER2*$^{-/-}$/*VLDLR*$^{-/-}$ and Dab$^{-/-}$ mice.

Because Reelin is not present in the SVZ or at the origin of the RMS, the inability of neuroblasts lacking ApoER2 and VLDLR to form chains must be Reelin-independent. This notion is in agreement with the explant assays performed here (Fig. 6). Interestingly, not only ApoER2 and/or VLDLR, but also their intracellular adapter Dab1 and at least one of the tyrosines that are phosphorylated upon Reelin stimulation, are needed for this function. Whether phosphorylation of Dab1 is necessary for proper chain formation or for other functions such as the ability of Dab1 to regulate cell surface expression of ApoER2 and VLDLR (34) is not clear yet. Mice lacking both receptors, lacking Dab1, or carrying the *Dab1-5F* alleles have identical phenotypes, characterized by massive accumulation of neuroblasts in the SVZ and the lack of stream formation, but development of the respective explants in Matrigel is different. A significant number of neuroblasts lacking Dab1 do migrate out of the explants but fail to form chains, whereas hardly any neuroblasts leave the explant derived from receptor-deficient mice, and the few chains formed are very short. This indicates that Dab1 is dispensable for migration but necessary for chain formation. Coculturing WT with *ApoER2*$^{-/-}$/*VLDLR*$^{-/-}$ explants demonstrated that (*i*) the presence of the WT explant did not alter the behavior of the mutant explant and (*ii*) none of the few cells leaving the mutant explant is incorporated into WT chains.

An important question concerns the putative ligands of this Reelin-independent function of the "receptor/Dab1" machinery in chain formation and/or migration. Such a ligand would be predicted not to act exactly like Reelin, because activation of the classical Reelin signaling pathway leads to dissociation of the chains (13). Here we have characterized F-spondin as an alternative ligand for ApoER2 and VLDLR present in the RMS. Whether it stimulates Dab1 phosphorylation like Reelin does, but lacks additional activity necessary for the full-blown Reelin signal (35), or whether it acts as substrate for neuroblasts to adhere to each other remains to be established.

The phenotype produced by the loss of components of the ApoER2/VLDLR/Dab1 complex is very similar to that seen in mice lacking SRF (5), in terms of both neuroanatomical abnormalities and the inability of SVZ explants to produce chains. *Srf*-negative mice show a dramatic reduction in brain levels of actin and gelsolin. Because none of the mice lacking components of the Reelin pathway exhibit altered levels of actin or gelsolin, we assume that the defect described here is independent of that produced by the lack of SRF.

In summary, we have identified a function of the ApoER2/VLDLR/Dab1 machinery that is independent of Reelin and mediates neuroblast migration and chain formation in the SVZ. Disruption of the machinery blocks postnatal neuronal migration from the SVZ to the OB and results in severe neuroanatomical defects in the OBs of affected mice.

Materials and Methods

Animals. WT mice on C57BL6/J or BalbC background, *reeler-Orleans* mice on a BalbC background (36), *Dab*$^{-/-}$ mice on a

C57Bl6/129Sv or BalbC background (22), *Dab1-5F* mice on a C57Bl6/129Sv or BalbC background (26), and *ApoER2*$^{-/-}$, *VLDLR*$^{-/-}$, and *ApoER2*$^{-/-}$/*VLDLR*$^{-/-}$ mice on a C57BL/6J/129Sv background were housed under standard conditions.

Histology and Immunohistochemistry. Animals were anesthetized with a combination of xylazine/ketamine (10 mg/kg and 75 mg/kg, respectively) in 0.9% NaCl and immediately perfused with 4% paraformaldehyde in PBS at 4°C. Brains were dehydrated and embedded in paraffin according to standard protocols. Serial coronal and sagittal paraffin sections (5 μm) were obtained and stained with hematoxylin following standard protocols. For immunohistochemistry dehydrated paraffin sections were heat-treated with EDTA buffer-CC1 (Ventana, Tucson, AZ) (pH 8.0) for 38 min at 95°C and incubated with the Discovery System (Ventana) to expose antigenic epitopes. The following primary antibodies were used: anti-doublecortin (C-18 goat polyclonal, 1:1,000; Santa Cruz Biotechnology, Santa Cruz, CA), anti-GFAP (rabbit polyclonal, 1:500; Dako, Glostrup, Denmark), anti-ApoER2 (no. 186 rabbit polyclonal, 1:1,000) (20), anti-calretinin and anti-calbindin (1:500; Sigma, St. Louis, MO), and anti-F-spondin (R2 and R4; a kind gift from Avihu Klar, Hebrew University, Hadassah Medical School, Jerusalem, Israel). Endogenous peroxidase activity was blocked, and chromogenic detection reaction was performed by using the DAB-Map kit (Ventana). Primary antibodies were visualized by incubating the sections with the respective antibodies for 1 h at room temperature [anti-goat secondary probe Alexa Fluor 488 (Molecular Probes) diluted 1:500 in PBS, anti-mouse Texas red (Molecular Probes) diluted 1:500 in PBS, and anti-rabbit Alexa Fluor 594 (Molecular Probes) diluted 1:500 in PBS].

Microscopy. Confocal images were acquired by using an LSM 5 system and LSM 5 software (Zeiss, Göttingen, Germany). Fluorescence and DIC images were acquired by using an Axiovert 135 system and AxioVision software (Zeiss).

BrdU Experiments and TUNEL Assay. Animals (P12) were injected i.p. with BrdU (50 mg/kg of body weight; Sigma) dissolved in 0.9% NaCl and killed at P17. BrdU stainings were performed on matched paraffin sections (5 μm) after 20 min of boiling in citrate buffer (pH 6) for antigen retrieval using anti-BrdU antibodies (Becton Dickinson, Mountain View, CA) diluted 1:50 in antibody dilution buffer (1% BSA/0.1% gelatin in PBS, pH 7.2). TUNEL assays were performed with the *In Situ* Cell Death Detection Kit (Roche Applied Biosciences).

SVZ Explants. SVZ explants were prepared as reported (4). Briefly, newborn pups were genotyped at P2–P3 and killed at P5 by decapitation. Brains were dissected and placed in cold OptiMEM (Gibco–Invitrogen, Carlsbad, CA). Slices (350 μm) were obtained by using a vibratome (Leica, Wetzlar, Germany). The SVZ was dissected from the lateral wall of the anterior horn of the lateral ventricle and cut into pieces of 250–350 μm in diameter. The explants were mixed with Matrigel (Becton Dickinson) and cultured in four-well dishes. After polymerization (20 min) 500 μl of serum-free medium supplemented with B-27 (Gibco–Invitrogen), 50 ng/ml insulin (Novo Nordisk, Graz, Austria), 100 μM putrescine (Sigma), 1 nM progesterone (Sigma), and glutamine and penicillin/Streptomycin (Gibco–Invitrogen) was added. Cultures were maintained in a humidified, 5% CO_2, 37°C incubator. After 50 h explants were monitored and the number of individual neurons per field and the length of migratory chains were measured by using AxioVision software (Zeiss). SVZ explants from WT mice were infected with Ad5CMV-eGFP (Gene Transfer Vector Core, University of Iowa, Iowa City, IA) with a titer of 1×10^{10} viral particles per milliliter in OptiMEM for 1 h in a humidified, 5% CO_2, 37°C incubator. Infected explants where washed three times with 10 volumes of OptiMEM, mixed with *ApoER2*$^{-/-}$/*VLDLR*$^{-/-}$ explants, and kept in culture under the same conditions described above.

Western Blots. Total protein extracts (20 μg) from forebrains (P17, derived from two mice each) were resolved by SDS/PAGE, and Western blotting was performed by using anti-gelsolin (goat polyclonal, 1:500; Santa Cruz Biotechnology), anti-actin (mouse monoclonal, 1:1,000; a kind gift from Vic Small, Institute of Molecular Biotechnology, Austrian Academy of Science, Vienna, Austria), and anti-Erk 1/2 (rabbit polyclonal, 1:10,000; Sigma) antibodies.

We thank Juan Guinea Viniegra for help with the TUNEL assay. This work was supported by the Fonds zur Förderung der Wissenschaftlichen Forschung Grants P16872-B09 and P19611-B09 and the Herzfelder'sche Familienstiftung.

1. Luskin MB (1993) *Neuron* 11:173–189.
2. Lois C, Alvarez-Buylla A (1994) *Science* 264:1145–1148.
3. Lois C, Garcia-Verdugo JM, Alvarez-Buylla A (1996) *Science* 271:978–981.
4. Wichterle H, Garcia-Verdugo JM, Alvarez-Buylla A (1997) *Neuron* 18:779–791.
5. Alberti S, Krause SM, Kretz O, Philippar U, Lemberger T, Casanova E, Wiebel FF, Schwarz H, Frotscher M, Schutz G, Nordheim A (2005) *Proc Natl Acad Sci USA* 102:6148–6153.
6. Tomasiewicz H, Ono K, Yee D, Thompson C, Goridis C, Rutishauser U, Magnuson T (1993) *Neuron* 11:1163–1174.
7. Chazal G, Durbec P, Jankovski A, Rougon G, Cremer H (2000) *J Neurosci* 20:1446–1457.
8. Hu H, Tomasiewicz H, Magnuson T, Rutishauser U (1996) *Neuron* 16:735–743.
9. Nguyen-Ba-Charvet KT, Picard-Riera N, Tessier-Lavigne M, Baron-Van Evercooren A, Sotelo C, Chedotal A (2004) *J Neurosci* 24:1497–1506.
10. Wu W, Wong K, Chen J, Jiang Z, Dupuis S, Wu JY, Rao Y (1999) *Nature* 400:331–336.
11. Murase S, Horwitz AF (2002) *J Neurosci* 22:3568–3579.
12. Petreanu L, Alvarez-Buylla A (2002) *J Neurosci* 22:6106–6113.
13. Hack I, Bancila M, Loulier K, Carroll P, Cremer H (2002) *Nat Neurosci* 5:939–945.
14. Perez-Garcia CG, Tissir F, Goffinet AM, Meyer G (2004) *Eur J Neurosci* 20:2827–2832.
15. Wyss JM, Stanfield BB, Cowan WM (1980) *Brain Res* 188:566–571.
16. Rice DS, Curran T (2001) *Annu Rev Neurosci* 24:1005–1039.
17. Tissir F, Goffinet AM (2003) *Nat Rev Neurosci* 4:496–505.
18. D'Arcangelo G, Homayoundi R, Keshvara L, Rice DS, Sheldon M, Curran T (1999) *Neuron* 24:471–479.
19. Hiesberger T, Trommsdorff M, Howell BW, Goffinet A, Mumby MC, Cooper JA, Herz J (1999) *Neuron* 24:481–489.
20. Strasser V, Fasching D, Hauser C, Mayer H, Bock HH, Hiesberger T, Herz J, Weeber EJ, Sweatt JD, Pramatarova A, *et al.* (2004) *Mol Cell Biol* 24:1378–1386.
21. D'Arcangelo G, Miao GG, Chen SC, Soares HD, Morgan JI, Curran T (1995) *Nature* 374:719–723.
22. Howell BW, Hawkes R, Soriano P, Cooper JA (1997) *Nature* 389:733–737.
23. Sheldon M, Rice DS, D'Arcangelo G, Yoneshima H, Nakajima K, Mikoshiba K, Howell BW, Cooper JA, Goldowitz D, Curran T (1997) *Nature* 389:730–733.
24. Trommsdorff M, Gotthardt M, Hiesberger T, Shelton J, Stockinger W, Nimpf J, Hammer R, Richardson JA, Herz J (1999) *Cell* 97:689–701.
25. Koizumi H, Higginbotham H, Poon T, Tanaka T, Brinkman BC, Gleeson JG (2006) *Nat Neurosci* 9:779–786.
26. Howell BW, Herrick TM, Hildebrand JD, Zhang Y, Cooper JA (2000) *Curr Biol* 10:877–885.
27. Paxinos G, Franklin KBJ (2003) *The Mouse Brain in Stereotaxic Coordinates* (Elsevier Academic, Amsterdam).
28. Takahara T, Ohsumi T, Kuromitsu J, Shibata K, Sasaki N, Okazaki Y, Shibata H, Sato S, Yoshiki A, Kusakabe M, Muramatsu M, *et al.* (1996) *Hum Mol Genet* 5:989–993.
29. Alcantara S, Ruiz M, D'Arcangelo G, Ezan F, de Lecea L, Curran T, Sotelo C, Soriano E (1998) *J Neurosci* 18:7779–7799.
30. Nimpf J, Schneider WJ (2000) *Biochim Biophys Acta* 1529:287–298.
31. Hoe HS, Wessner D, Beffert U, Becker AG, Matsuoka Y, Rebeck GW (2005) *Mol Cell Biol* 25:9259–9268.
32. Lein ES, Hawrylycz MJ, Ao N, Ayres M, Bensinger A, Bernard A, Boe AF, Boguski MS, Brockway KS, Byrnes EJ, *et al.* (2007) *Nature* 445:168–176.
33. Simo S, Pujadas L, Segura MF, La Torre A, Del Rio JA, Urena JM, Comella JX, Soriano E (2007) *Cereb Cortex* 17:294–303.
34. Morimura T, Hattori M, Ogawa M, Mikoshiba K (2005) *J Biol Chem* 280:16901–16908.
35. Jossin Y, Ignatova N, Hiesberger T, Herz J, Lambert de Rouvroit C, Goffinet AM (2004) *J Neurosci* 24:514–521.
36. de Bergeyck V, Nakajima K, Lambert de Rouvroit C, Naerhuyzen B, Goffinet AM, Miyata T, Ogawa M, Mikoshiba K (1997) *Brain Res Mol Brain Res* 50:85–90.